Comparative Study of the Reactions of Diazomethane with μ_3-Imidoyl and μ_3-Butyne Trinuclear Clusters

Michael Day, William Freeman, Kenneth I. Hardcastle, Mark Isomaki, Shariff E. Kabir, Tim McPhillips, Edward Rosenberg,* Lincoln G. Scott, and Erich Wolf

Department of Chemistry, California State University, Northridge, California 91330

Received September 23, 1991

The reaction of the μ_3-imidoyl clusters $(\mu\text{-H})(\mu_3\text{-}\eta^2\text{-CH}_3\text{C}{=}\text{NCH}_2\text{CH}_3)\text{Ru}_3(\text{CO})_9$ (1), $(\mu\text{-H})(\mu_3\text{-}\eta^2\text{-C}{=}\text{NCH}_2\text{CH}_2\text{CH}_2)\text{Os}_3(\text{CO})_9$ (2), and $(\mu\text{-H})(\mu_3\text{-}\eta^2\text{-CH}_3\text{CH}_2\text{C}{=}\text{NCH}_2\text{CH}_2\text{CH}_3)\text{Os}_3(\text{CO})_9$ (3) with CH_2N_2 at 25 °C yield the structurally analogous clusters $(\mu\text{-H})_2(\mu_3\text{-}\eta^2\text{-CH(CH}_3)\text{C}{=}\text{NCH}_2\text{CH}_3)\text{Ru}_3(\text{CO})_9$ (4), $(\mu\text{-H})_2(\mu_3\text{-}\eta^2\text{-CHC}{=}\text{NCH}_2\text{CH}_2\text{CH}_2)\text{Os}_3(\text{CO})_9$ (5), and $(\mu\text{-H})_2(\mu_3\text{-}\eta^2\text{-CH(CH}_3\text{CH}_2)\text{C}{=}\text{NCH}_2\text{CH}_2\text{CH}_3)\text{Os}_3(\text{CO})_9$ (6), in which a methylene fragment has inserted into the carbon-metal σ bond of the imidoyl ligand and undergone a C-H oxidative addition. The reaction of 1 with CD_2N_2 yields 4 with no hydrogen incorporation into the methyne hydrogen position. The reaction of 2-methylpyrrolidine with $\text{Os}_3(\text{CO})_{10}(\text{CH}_3\text{CN})_2$ gives $(\mu\text{-H})(\mu\text{-}\eta^2\text{-C}{=}\text{NCH(CH}_3)\text{CH}_2\text{CH}_2)\text{Os}_3(\text{CO})_{10}$ (7) and $(\mu\text{-H})(\mu\text{-}\eta^2\text{-CH}_2\text{C}{=}\text{NCH}_2\text{CH}_2\text{CH}_2)\text{Os}_3(\text{CO})_{10}$ (8) as the two major products. On thermolysis 8 converts quantitatively to 5 suggesting that a nonacarbonyl analog of 8 may be an intermediate in the reaction of 2 with CH_2N_2. The reaction of the related alkyne complex $(\mu\text{-CO})(\mu_3\text{-}\eta^2\text{-CH}_3\text{C}_2\text{CH}_3)\text{Os}_3(\text{CO})_9$ (9) with CH_2N_2 at 25 °C yields the methylene complex $(\mu\text{-CH}_2)(\mu_3\text{-}\eta^2\text{-CH}_3\text{C}_2\text{CH}_3)\text{Os}_3(\text{CO})_9$ (10, 59%) and $(\mu_3\text{-}\eta^1\text{-CH}_2\text{N}_2)(\mu_3\text{-}\eta^2\text{-CH}_3\text{C}_2\text{CH}_3)\text{Os}_3(\text{CO})_9$ (11, 22%). Compound 11 is a $50e^-$ cluster with two metal-metal bonds and one nitrogen atom capping the cluster. Compound 10 undergoes carbon-carbon coupling and C-H oxidative addition only at elevated temperatures (128 °C) to yield $(\mu\text{-H})(\mu_3\text{-}\eta^3\text{-CH}_3\text{CC(CH}_3)\text{CH})\text{Os}_3(\text{CO})_9$ (12). Compound 11 converts to 10 photochemically. This sequence of reactions was previously reported but as starting from the coordinatively unsaturated alkyne cluster $(\mu_3\text{-}\eta^2\text{-C}_6\text{H}_5\text{C}_2\text{C}_6\text{H}_5)\text{Os}_3(\text{CO})_9$. Solid-state structures for 4, 5, 10, and 11 are reported. Compound 4 crystallizes in the monoclinic space group $C2/c$ with $a = 16.997$ (3) Å, $b = 8.941$ (1) Å, $c = 27.322$ (6) Å, $\beta = 97.62$ (1)°, $V = 4115$ (2) Å^3, and $Z = 8$. Least-squares refinement of 2851 observed reflections gave a final agreement factor of $R = 0.026$ ($R_w = 0.035$). Compound 5 crystallizes in the triclinic space group $P\bar{1}$ with $a = 13.394$ (8) Å, $b = 15.601$ (8) Å, $c = 9.069$ (7) Å, $\alpha = 88.51$ (5)°, $\beta = 80.61$ (6)°, $\gamma = 86.96$ (5)°, $V = 1867$ (3) Å^3 at −158 °C, and $Z = 4$. Least-squares refinement of 6576 observed reflections gave a final agreement factor of $R = 0.070$ ($R_w = 0.090$). Compound 10 crystallizes in the triclinic space group $P\bar{1}$ with $a = 12.117$ (2) Å, $b = 16.793$ (3) Å, $c = 9.229$ (2) Å, $\alpha = 95.42$ (2)°, $\beta = 92.77$ (2)°, $\gamma = 92.79$ (1)°, $V = 1865$ (1) Å^3, and $Z = 4$. Least-squares refinement of 5807 observed reflections gave a final agreement of $R = 0.067$ ($R_w = 0.079$). Compound 11 crystallizes in the monoclinic space group $P2_1/c$ with $a = 9.245$ (2) Å, $b = 13.813$ (3) Å, $c = 16.202$ (3) Å, $\beta = 110.18$ (2)°, $V = 1942$ (1) Å^3, and $Z = 4$. Least-squares refinement of 3478 observed reflections gave a final agreement factor of $R = 0.040$ ($R_w = 0.047$).

Introduction

Carbon-carbon coupling processes on transition metal centers are of fundamental importance to our understanding of catalytic processes such as the Fischer-Tropsch reaction.[1-3] The pioneering work of Pettit and co-workers showed that the coupling of methylene fragments was a primary reaction pathway in building longer hydrocarbons from C_1 and C_2 fragments.[1,4] Recently there have been several reports of the coupling of μ_3-alkynes[5-7] with μ-methylenes or η^1-carbenes[8] in trinuclear clusters of osmium and ruthenium. In the case of osmium clusters, these reactions occur at elevated temperatures (68-135 °C) and are often associated with a carbon-hydrogen bond activation of the alkyne or the C_1 fragment.[5,8] For ruthenium, coupling of a μ-methylidyne[6] with uncoordinated alkynes at elevated temperatures (60 °C) and direct coupling of a methylene (from diazomethane) with a μ_3-alkyne[7] at room temperature have been reported. We recently reported the synthesis of a series of μ_3-imidoyl clusters of ruthenium and osmium: $(\mu\text{-H})(\mu_3\text{-}\eta^2\text{-CH}_3\text{C}{=}\text{NCH}_2\text{CH}_3)\text{Ru}_3(\text{CO})_9$ (1),[9] $(\mu\text{-H})(\mu_3\text{-}\eta^2\text{-C}{=}\text{NCH}_2\text{CH}_2\text{CH}_2)\text{Os}_3(\text{CO})_9$ (2),[10] and $(\mu\text{-H})(\mu_3\text{-}\eta^2\text{-CH}_3\text{CH}_2\text{C}{=}\text{NCH}_2\text{CH}_2\text{CH}_3)\text{Os}_3(\text{CO})_9$ (3).[10] We have found these valence saturated clusters to be remarkably reactive toward a range of two-electron donors[10b-12] (eqs 1-3).

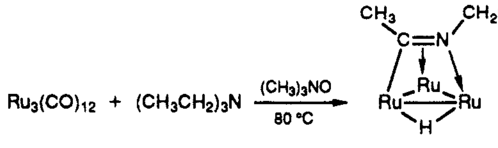

1

(1)

---

[1] Brady, R. C., III; Pettit, R. *J. Am. Chem. Soc.* **1981**, *103*, 1287.

[2] Laws, W. J.; Puddephatt, R. J. *J. Chem. Soc., Chem. Commun.* **1984**, 116.

[3] Herrmann, W. A. *Angew. Chem., Int. Ed. Engl.* **1982**, *21*, 117.

[4] (a) Brady, R. C., III; Pettit, R. *J. Am. Chem. Soc.* **1980**, *102*, 6181. (b) Summer, C. E., Jr.; Collier, J. A.; Pettit, R. *Organometallics* **1982**, *1*, 1350. (c) Summer, C. E., Jr.; Riley, P. E.; Davis, R. E.; Pettit, R. *J. Am. Chem. Soc.* **1980**, *102*, 1752.

[5] (a) Clauss, A. D.; Shapley, J. R.; Wilson, S. R. *J. Am. Chem. Soc.* **1981**, *103*, 7387. (b) Clauss, A. D. Ph.D. Thesis, University of Illinois, 1983.

[6] Beanan, L. R.; Keister, J. B. *Organometallics* **1985**, *4*, 1713.

[7] Nucciarone, D.; Taylor, N. J.; Carty, A. J. *Organometallics* **1984**, *3*, 177.

[8] (a) Adams, R. D.; Chen, G. *Organometallics* **1990**, *9*, 2882. (b) Adams, R. D.; Chen, G. *Organometallics* **1992**, *11*, 837.

[9] Aime, S.; Gobetto, R.; Padovan, F.; Botta, M.; Rosenberg, E.; Gellert, R. W. *Organometallics* **1987**, *6*, 2074.

[10] (a) Rosenberg, E.; Kabir, S. E.; Hardcastle, K. I.; Day, M.; Wolf, E. *Organometallics* **1990**, *9*, 2214. (b) Day, M.; Espitia, D.; Hardcastle, K. I.; McPhillips, T.; Kabir, S. E.; Rosenberg, E. *Inorg. Chem.*, submitted for publication.

[11] Day, M.; Espitia, D.; Hardcastle, K. I.; Kabir, S. E.; Rosenberg, E.; Gobetto, R.; Milone, L.; Osella, D. *Organometallics* **1991**, *10*, 3550.

0276-7333/92/2311-3376$03.00/0

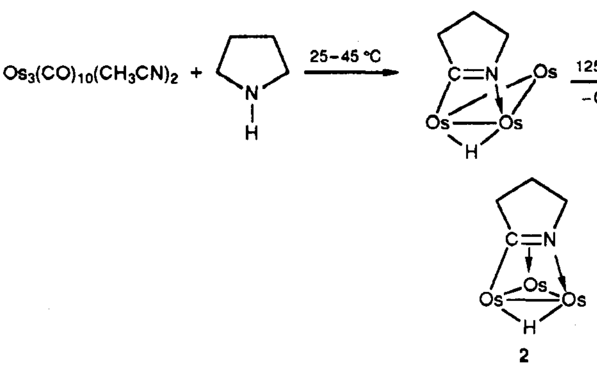

(2)

2

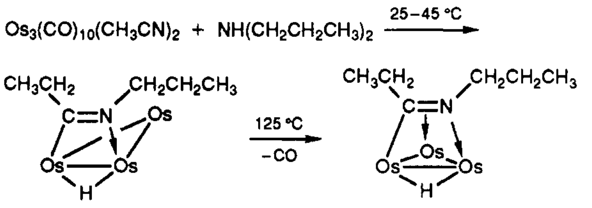

(3)

3

We report here the reactions of these highly reactive $48e^-$ clusters with diazomethane, where we observe carbon–carbon coupling and carbon–hydrogen bond activation at 0–25 °C with both the osmium and ruthenium clusters. We also report the reaction of CH_2N_2 with a related $48e^-$ μ_3-butynyl complex in order to compare its reactivity with that of 2.

Results and Discussion

The reaction of 1 with excess diazomethane at (0–25 °C) in diethyl ether yields a single trinuclear product, $(\mu\text{-H})_2(\mu_3\text{-}\eta^2\text{-CH(CH}_3)\text{C=NCH}_2\text{CH}_3)\text{Ru}_3(\text{CO})_9$ (eq 4), in 30% yield. The reaction is actually almost quantitative with respect to consumed 1 since virtually all the unreacted starting material is recovered. The only detectable side reaction is the polymerization of the diazomethane, which is apparently catalyzed by the cluster. All attempts to optimize the yield of 4, including gradual addition of diazomethane to 1, addition of 1 to excess diazomethane, and lowering the temperature to 0 °C were unsuccessful. Compound 4 was characterized by ^1H NMR, infrared spectroscopy, and elemental analysis. However, the exact bonding mode of the organic ligand to the trinuclear cluster and the relative disposition of the hydrides could not be deduced from these data and so a single-crystal X-ray crystallographic investigation was undertaken.

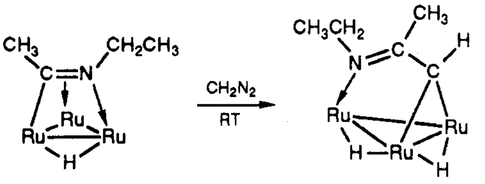

(4)

1

4

The solid-state structure of 4 is shown in Figure 1, crystal data are given in Table I, selected distances and bond angles appear in Table II, and atom coordinates appear in in Table III. The structure consists of an Ru_3 triangle with two almost equal metal–metal bonds (Ru(1)–Ru(3) = 2.7863 (5) and Ru(1)–Ru(2) = 2.7713 (6) Å) and one elongated metal–metal bond (Ru(2)–Ru(3) = 2.9567 (5) Å). The μ-alkylidene carbon bridges Ru(1) and Ru(3) symmetrically (Ru(1)–C(1) = 2.145 (5), Ru(3)–C(1) = 2.148 (5) Å), and the nitrogen is coordinated to Ru(2) with a bond length which is significantly longer than the lone pair–ruthenium interaction in 1 (Ru(3)–N = 2.08 (1) Å in 1[9] and Ru(2)–N = 2.123 (4) Å in 4). The C(2)–Ru distances in 4 (Ru(3)–C(2) = 3.080 (5), Ru(2)–C(2) = 2.950 (5) Å) preclude any bonding interaction between this atom and the cluster. Similarly, the C(2)–N double-bond distance of 1.297 (6) Å suggests that there is little π-interaction with the metal core. Thus the ligand donates four electrons to the metal core, and with the two hydrides, this makes 4 a saturated $48e^-$ cluster. The hydride ligand positions were estimated using the program HYDEX.[13] One hydride, H(2), shares the same edge as the alkylidene carbon and is tucked well below the Ru_3 triangle. The Ru(1)–Ru(3)–H(2) plane makes an angle of 70° with the Ru_3 plane. This arrangement is typical for a hydride sharing an edge with a one carbon atom bridge.[14,15] The other hydride, H(1), is located at the elongated Ru(2)–Ru(3) edge and is in plane with the Ru_3 triangle. The relative disposition of the two hydride ligands in 4 is similar to that of related dihydride ruthenium clusters containing μ_3-alkyne ligands.[16]

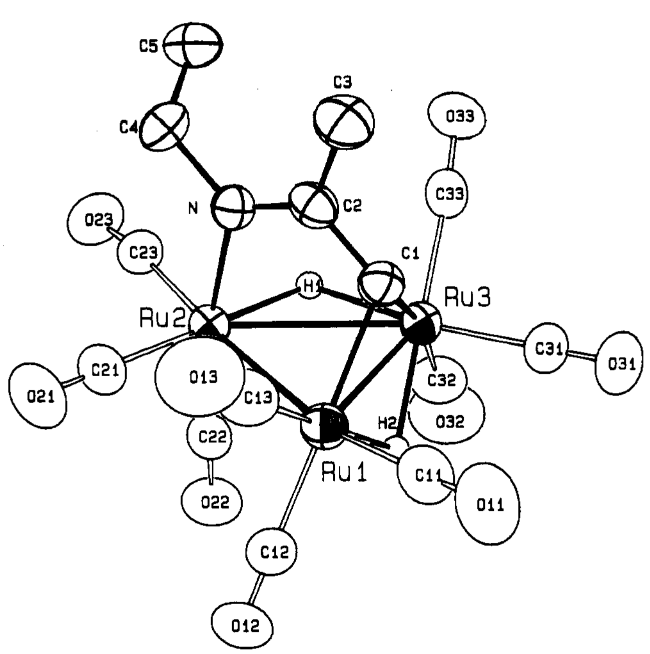

Figure 1. ORTEP diagram of $(\mu\text{-H})_2(\mu_3\text{-}\eta^2\text{-CH(CH}_3)\text{C=NCH}_2\text{CH}_3)\text{Ru}_3(\text{CO})_9$ (4), showing the calculated positions of the hydrides.

There are several possible pathways by which 4 can form from 1 and diazomethane. Stable diazomethane adducts of polynuclear carbonyl complexes have been reported,[5] and it seems likely that coordination of an intact diazomethane to a metal site is the first step in the reaction since we have shown that complexes such as 1–3 are sus-

---

(12) (a) Rosenberg, E.; Hardcastle, K. I.; Day, M.; Hajela, S.; Wolf, E.; Milone, L.; Gobetto, R. *Abstracts*, Pacifichem Meeting, Honolulu, HI, Dec 17–22, 1989; American Chemical Society: Washington, DC, 1989. (b) Day, M.; Hajela, S.; Hardcastle, K. I.; McPhillips, T.; Rosenberg, E.; Botta, M.; Gobetto, R.; Milone, L.; Gellert, R. W. *Organometallics* **1990**, *9*, 913.

(13) Orpen, A. G. *J. Chem. Soc., Dalton Trans.* **1980**, 2059.

(14) Catti, M.; Gervasio, G.; Mason, S. A. *J. Chem. Soc., Dalton Trans.* **1977**, 2260.

(15) (a) Jangala, C.; Rosenberg, E.; Skinner, D.; Aime, S.; Milone, L.; Sappa, E. *Inorg. Chem.* **1980**, *19*, 1571. (b) Day, M.; Hajela, S.; Kabir, S. E.; Irving, M.; McPhillips, T.; Wolf, E.; Hardcastle, K. I.; Rosenberg, E.; Gobetto, R.; Milone, L.; Osella, D. *Organometallics* **1991**, *10*, 2743.

(16) (a) Churchill, M. R.; Fettinger, J. C.; Keister, J. B.; See, R.; Ziller, J. W. *Organometallics* **1985**, *4*, 2112. (b) Janik, T. S.; Churchill, M. R.; Duggan, T. P.; Keister, J. B. *J. Organomet. Chem.* **1988**, *353*, 343. (c) Churchill, M. R.; Janik, T. S.; Duggan, T. P.; Keister, J. B. *Organometallics* **1987**, *6*, 799. (d) Nevinger, L. R.; Keister, J. B. *Organometallics* **1990**, *9*, 2312.

Table I. Crystal Data: Collection and Refinement Parameters

compd	4	5	10	11
formula	$C_{14}H_{11}NO_9Ru_3$	$C_{14}H_9NO_9Os_3$	$C_{14}H_8O_9OS_3$	$C_{14}H_8N_2O_9Os_3$
fw	640.46	905.83	890.81	918.83
cryst system	monoclinic	triclinic	triclinic	monoclinic
space group	$C2/c$	$P\bar{1}$	$P\bar{1}$	$P2_1/c$
a, Å	16.997 (3)	13.394 (8)	12.117 (2)	9.245 (2)
b, Å	8.941 (1)	15.601 (8)	16.793 (3)	13.813 (3)
c, Å	27.322 (6)	9.069 (7)	9.229 (2)	16.202 (3)
α, deg		88.51 (5)	95.42 (2)	
β, deg	97.62 (1)	80.61 (6)	92.77 (2)	110.18 (2)
γ, deg		86.96 (5)	92.79 (1)	
V, Å^3	4115 (2)	1867 (3)	1865 (1)	1942 (1)
Z	8	4	4	4
D_{calc}, g/cm^3	2.07	3.22	3.17	3.14
abs coeff μ, cm^{-1}	21.8	195.7	204.7	196.6
data collect temp, °C	25 ± 1	−158 ± 1	25 ± 1	25 ± 1
radiation	Mo Kα	Mo Kα	Mo Kα	Mo Kα
scan mode	ω–2θ	ω–2θ	ω–2θ	ω–2θ
scan limits, deg	$2 < 2\theta < 48°$	$2 < 2\theta < 52$	$2 < 2\theta < 50$	$2 < 2\theta < 54$
scan speed, deg/min	8.2	8.2	8.2	8.2
scan range, deg	0.8	0.8	0.8	0.9
no. of data collecd	3461	16491	6549	4419
no. of data obsd	2851	6576	5807	3478
no. of variables	244	247	379	253
R^a	0.026	0.070	0.067	0.040
$R_w{}^b$	0.035	0.090	0.079	0.047
largest shift/esd	0.01	0.03	0.01	
weighting scheme	$1/\sigma^2$	$1/\sigma^2$	$1/\sigma^2$	$1/\sigma^2$
highest peak in final diff map, eÅ^{-3}	0.56 (6)	4.88 (75)	3.17 (67)	1.28 (43)
relative transm coeff	0.79–1.00	0.67–0.99	0.24–1.00	0.49–1.00

[a] $R = \sum||F_o| - |F_c||/\sum|F_o|$. [b] $R_w = [(\sum w(|F_o| - |F_c|)^2/\sum w|F_o|^2]^{1/2}$.

Table II. Selected Distances (Å) and Angles (deg) for $(\mu\text{-H})_2(\mu_3\text{-}\eta^2\text{-CH(CH}_3\text{)C=NCH}_2\text{CH}_3\text{)Ru}_3\text{(CO)}_9$ (4)[a]

	Distances		
Ru(1)–Ru(2)	2.7713 (6)	Ru(2)–N	2.950 (5)
Ru(1)–Ru(3)	2.7863 (5)	Ru(3)–C(2)	3.080 (5)
Ru(2)–Ru(3)	2.9567 (5)	N–C(2)	1.297 (6)
Ru(1)–C(1)	2.145 (5)	C(2)–C(3)	1.531 (7)
Ru(3)–C(1)	2.148 (5)	C(1)–C(2)	1.453 (7)
Ru(2)–N	2.123 (4)	N–C(4)	1.491 (6)
Ru(2)–H(1)	1.85	C(4)–C(5)	1.542 (8)
Ru(3)–H(1)	1.85	Ru–C(CO)	1.91 (3)*
Ru(1)–H(2)	1.85	C–O(CO)	1.13 (1)*
Ru(3)–H(2)	1.85		
	Angles		
Ru(1)–Ru(2)–Ru(3)	58.11 (1)	C(1)–C(2)–C(3)	116.9 (5)
Ru(1)–Ru(3)–Ru(2)	57.61 (1)	C(2)–N–C(4)	120.8 (4)
Ru(2)–Ru(1)–Ru(3)	64.28 (1)	N–C(2)–C(1)	119.9 (4)
Ru–C–O(CO)	177 (1)*	N–C(2)–C(3)	123.2 (5)
		N–C(4)–C(5)	110.5 (5)

[a] Numbers in parentheses are estimated standard deviations in the least significant digits. Asterisks indicate average values.

Table III. Fractional Atomic Coordinates for $(\mu\text{-H})_2(\mu_3\text{-}\eta^2\text{-CH(CH}_3\text{)C=NCH}_2\text{CH}_3\text{)Ru}_3\text{(CO)}_9$ (4)

atom	x	y	z	B,[a] Å^2
Ru(1)	0.23007 (2)	0.57114 (4)	0.08166 (1)	4.535 (9)
Ru(2)	0.15795 (2)	0.55329 (4)	0.16668 (1)	3.881 (8)
Ru(3)	0.28006 (2)	0.33608 (4)	0.14524 (1)	4.130 (8)
O(11)	0.3203 (4)	0.5117 (6)	−0.0039 (2)	11.9 (2)
O(12)	0.2987 (3)	0.8854 (4)	0.0998 (2)	8.0 (1)
O(13)	0.0774 (3)	0.6548 (6)	0.0184 (2)	12.6 (2)
O(21)	0.0585 (3)	0.8217 (5)	0.1289 (2)	9.3 (1)
O(22)	0.2914 (2)	0.7465 (4)	0.2161 (1)	6.30 (9)
O(23)	0.0928 (2)	0.5241 (5)	0.2654 (1)	6.72 (9)
O(31)	0.3859 (2)	0.1926 (5)	0.0780 (2)	8.9 (1)
O(32)	0.4080 (3)	0.3956 (5)	0.2333 (2)	9.1 (1)
O(33)	0.2115 (2)	0.0473 (4)	0.1788 (2)	6.9 (1)
N	0.0800 (2)	0.3983 (4)	0.1264 (1)	4.34 (8)
C(1)	0.1890 (3)	0.3444 (5)	0.0828 (2)	4.5 (1)
C(2)	0.1083 (3)	0.3194 (5)	0.0929 (2)	4.5 (1)
C(3)	0.0608 (3)	0.1969 (6)	0.0630 (2)	6.6 (1)
C(4)	−0.0020 (3)	0.3719 (6)	0.1382 (2)	5.9 (1)
C(5)	−0.0029 (4)	0.2401 (7)	0.1746 (2)	7.0 (1)
C(11)	0.2858 (4)	0.5346 (7)	0.0279 (2)	7.1 (1)
C(12)	0.2730 (3)	0.7700 (6)	0.0934 (2)	5.6 (1)
C(13)	0.1353 (4)	0.6268 (7)	0.0423 (2)	7.5 (2)
C(21)	0.0955 (3)	0.7212 (6)	0.1422 (2)	5.8 (1)
C(22)	0.2404 (3)	0.6771 (5)	0.1969 (2)	4.6 (1)
C(23)	0.1144 (3)	0.5249 (5)	0.2277 (2)	4.8 (1)
C(31)	0.3477 (3)	0.2447 (6)	0.1037 (2)	6.0 (1)
C(32)	0.3619 (3)	0.3726 (6)	0.2009 (2)	6.0 (1)
C(33)	0.2393 (3)	0.1521 (5)	0.1660 (2)	4.9 (1)
H(1)	0.220	0.396	0.193	4.0*
H(2)	0.319	0.515	0.124	4.0*

[a] Starred B values are for atoms that were refined isotropically. Anisotropically refined atoms are given in the form of the isotropic equivalent displacement parameter defined as $(4/3)[a^2B(1,1) + b^2B(2,2) + c^2B(3,3) + ab(\cos\gamma)B(1,2) + ac(\cos\beta)B(1,3) + bc(\cos\alpha)B(2,3)]$.

ceptible to nucleophilic attack at room temperature by two-electron donors to give $(\mu\text{-H})(\mu_3\text{-imidoyl})\text{Ru}_3\text{(CO)}_8\text{L}$ (L = phosphine or isocyanide) substitution products[12] or $(\mu\text{-H})(\mu\text{-imidoyl})\text{Os}_3\text{(CO)}_9\text{L}$ addition products.[10b,11] The initial diazomethane adduct is apparently quite unstable, as we observe gas evolution and polymer formation, presumably N_2 and polymethylene (identified by infrared spectroscopy), immediately upon addition of 1 to ethereal solutions of diazomethane. We tentatively exclude the formation of a stable $(\mu\text{-H})(\mu\text{-CH}_2)(\mu\text{-imidoyl})\text{Ru}_3\text{(CO)}_9$ complex on the basis of a reaction performed with CD_2N_2. Shapley et al. previously reported the isolation of $(\mu_3\text{-}\eta^1\text{-CH}_2\text{N}_2)(\mu_3\text{-}\eta^2\text{-C}_6\text{H}_5\text{C}_2\text{C}_6\text{H}_5)\text{Os}_3\text{(CO)}_9$ and $(\mu\text{-CH}_2)(\mu_3\text{-}\eta^2\text{-C}_6\text{H}_5\text{C}_2\text{C}_6\text{H}_5)\text{Os}_3\text{(CO)}_9$ from the reaction of the coordinatively unsaturated $(\mu_3\text{-}\eta^2\text{-C}_6\text{H}_5\text{C}_2\text{C}_6\text{H}_5)\text{Os}_3\text{(CO)}_9$ with diazomethane.[5] Earlier, Shapley and co-workers also reported the isolation of $(\mu\text{-H})_2(\mu\text{-CH}_2)\text{Os}_3\text{(CO)}_{10}$ from the reaction of $(\mu\text{-H})_2\text{Os}_3\text{(CO)}_{10}$ with diazomethane.[17] This dihydrido–μ-methylene complex exists in equilibrium with $(\mu\text{-H})(\mu\text{-CH}_3)\text{Os}_3\text{(CO)}_{10}$, and rapid hydrogen deuterium scrambling is observed when diazomethane is reacted with

---

(17) Calvert, R. B.; Shapley, J. R. *J. Am. Chem. Soc.* **1977**, *99*, 5225.

Scheme I

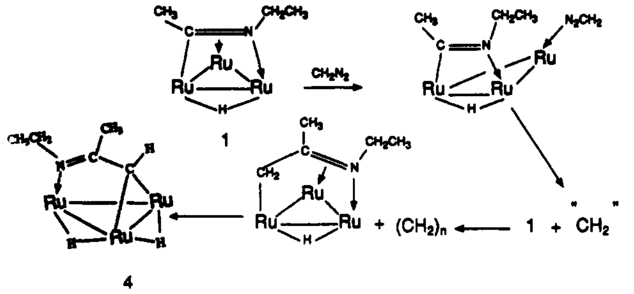

(μ-D)$_2$Os$_3$(CO)$_{10}$.[18] We reacted CD$_2$N$_2$ with 1 and observed no incorporation of hydrogen into the alkylidene C–H in the 4 formed and about 50% deuterium incorporated into both hydride positions in 4. This result requires that C–D bond cleavage is irreversible but does not exclude a relatively short-lived μ-hydrido–μ-methylene complex as an intermediate and favors dissociative formation of methylene followed by direct insertion of methylene into the carbon–metal bond followed by C–H oxidative addition to yield 4 (Scheme I). A direct analog of the proposed intermediate insertion product (Scheme I) is obtained as one of four products from the reaction of Ru$_3$(CO)$_{12}$ with NEt$_3$[12b] (eq 5). The coordination mode of CH$_2$N$_2$ to the clusters when it decomposes is not known but probably is more complex than the simple η^1-axial coordination shown in Scheme I. Another possibility, related to that shown in Scheme I, is direct attack by diazomethane on the bridging imidoyl carbon followed by nitrogen loss and rearrangement.

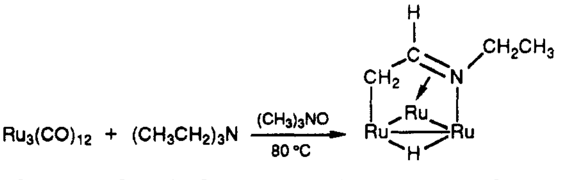
(5)

Consistent with this suggested reaction pathway is the fact that (μ-H)(μ-η^2-CH$_3$C=NCH$_2$CH$_3$)Ru$_3$(CO)$_{10}$ (made by CO addition of 1[12]) decomposes diazomethane much more slowly than 1, with only slow formation of polymer observed. This suggests that dissociation of CO is necessary before cluster-catalyzed decomposition of diazomethane and competitive formation of 4 can take place. This result does not, however, exclude the possibility of direct attack of diazomethane on the imidoyl carbon in 1 since the μ- and μ_3-imidoyl carbon may have different reactivities.

In general, organometallic osmium clusters are less reactive than their ruthenium analogs. This is also true for the relatively reactive μ_3-imidoyl clusters 1–3, where for osmium[10b,11] ligand addition occurs at room temperature while for ruthenium[12] ligand addition occurs even at −80 °C. For this reason we thought it might be useful to examine the reactions of 2 and 3 with diazomethane in the hope of perhaps stabilizing an intermediate not observed for 1. Interestingly, both 2 and 3 react at room temperature with diazomethane to give the directly analogous complexes (μ-H)$_2$(μ_3-η^2-CH$\overline{\mathrm{C{=}NCH_2CH_2C}}H_2$)Os$_3(CO)_9$ (5) and (μ-H)$_2$(μ_3-η^2-CH(CH$_3$CH$_2$)C=NCH$_2$CH$_2$CH$_3$)Os$_3$(CO)$_9$ (6), respectively (eqs 6 and 7).

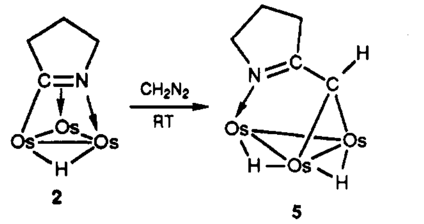
(6)

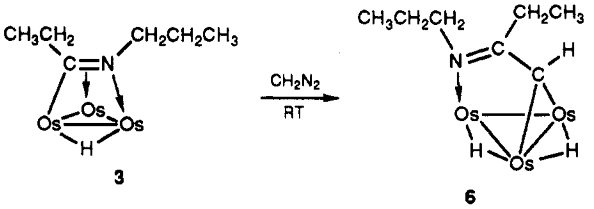
(7)

The yields obtained for 5 and 6 are very poor and significantly lower than for 4, but as for 4, unreacted starting material is recovered almost quantitatively and the only byproduct is polymethylene. As for the synthesis of 4 from 1, addition of aliquots of ethereal solutions of diazomethane to solutions of 2 or 3 in various solvents (ether, dichloromethane, hexane, benzene) over a range of temperatures (0–42 °C) did not appreciably increase the yield.

Compound 5 can also be synthesized by the two-step process of reaction of 2-methylpyrrolidine with Os$_3$(CO)$_{10}$(CH$_3$CN)$_2$ at +50 °C, which yields the μ-imidoyl derivative μ-H(μ-η^2-$\overline{\mathrm{C{=}NCH(CH_3)CH_2C}}H_2$)Os$_3(CO)_{10}$ (7) and μ-H(μ-η^2-CH$_2\overline{\mathrm{C{=}NCH_2CH_2C}}H_2$)Os$_3(CO)_{10}$ (8) as the two major products, followed by thermolysis of 8, which converts to 5 quantitatively at 100 °C in 23 h (eqs 8 and 9). This result seems to support the initial formation of HOs$_3$(CO)$_9$(μ- or μ_3-CH$_2\overline{\mathrm{C{=}NCH_2CH_2C}}H_2$) in the reaction of 2 with CH$_2$N$_2$, as suggested for 1 reacting with CH$_2$N$_2$ in Scheme I.

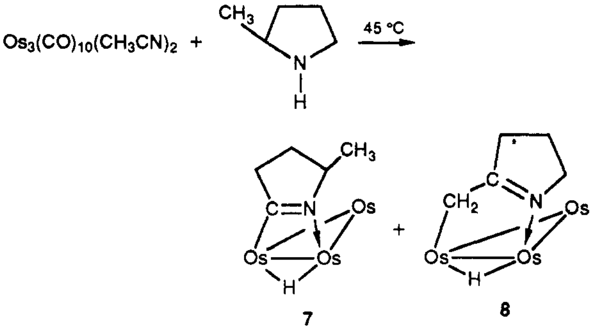
(8)

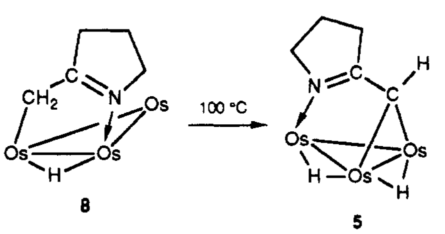
(9)

The solid-state structure of 5 is illustrated in Figure 2, crystal data are given in Table I, selected distances and bond angles are given in Table IV, and fractional coordinates are given in Table V. Compound 5 crystallizes with two almost identical molecules in the asymmetric unit. The structure of molecule A consists of a trimetallic core with two almost equivalent metal–metal bonds (Os(1)–Os(2) = 2.810 (1), Os(2)–Os(3) = 2.812 (1) Å) and one elongated metal–metal bond (Os(1)–Os(3) = 3.005 (1) Å; in molecule B the respective distances are Os(1B)–Os(2B) = 2.999 (1), Os(2B)–Os(3B) = 2.802 (1), and Os(1B)–Os(3)

---

(18) Calvert, R. B.; Shapley, J. R. *J. Am. Chem. Soc.* **1978**, *100*, 7726.

(19) (a) Nucciarone, D.; Taylor, N. J.; Carty, A. J. *Organometallics* **1986**, *5*, 1179. (b) Johnson, B. F. G.; Lewis, J.; Raithby, P. R.; Sankey, S. W. *J. Organomet. Chem.* **1982**, *231*, C65. (c) Keijsper, J.; Polm, L. H.; van Koten, G.; Vrieze, K.; Goubitz, K.; Stam, C. H. *Organometallics* **1985**, *4*, 1876.

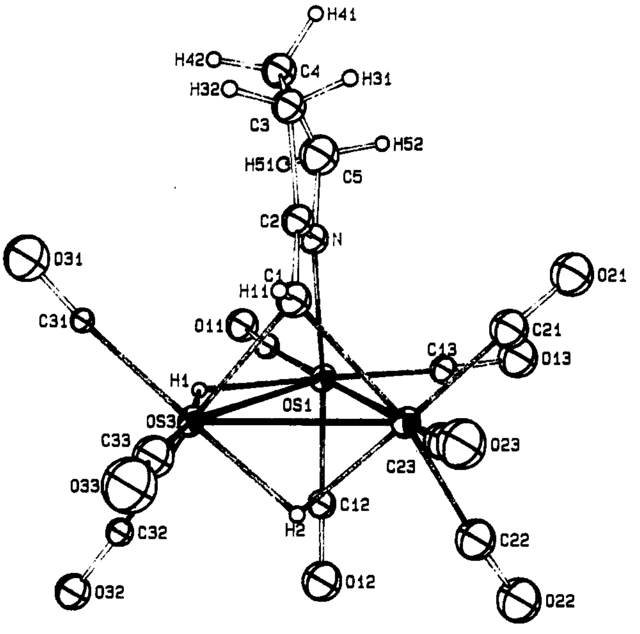

Figure 2. ORTEP diagram of $(\mu\text{-H})_2(\mu_3\text{-}\eta^2\text{-CH}\overline{\text{C=NCH}_2\text{CH}_2\text{C}}\text{H}_2)\text{Os}_3(\text{CO})_9$ (5), molecule A, showing the calculated positions of the hydrides.

Table IV. Selected Distances (Å) and Angles (deg) for $(\mu\text{-H})_2(\mu_3\text{-}\eta^2\text{-CH}\overline{\text{C=NCH}_2\text{CH}_2\text{C}}\text{H}_2)\text{Os}_3(\text{CO})_9$ (5)[a]

	Distances		
Os(1)–Os(2)	2.810 (1)	Os(1B)–Os(2B)	2.999 (1)
Os(1)–Os(3)	3.005 (1)	Os(1B)–Os(3B)	2.808 (1)
Os(2)–Os(3)	2.812 (1)	Os(2B)–Os(3B)	2.802 (1)
Os(1)–N	2.10 (2)	Os(1B)–N(B)	2.13 (2)
Os(2)–C(1)	2.19 (2)	Os(2B)–C(1B)	2.18 (2)
Os(3)–C(1)	2.14 (2)	Os(3B)–C(1B)	2.15 (2)
N–C(2)	1.28 (2)	N(B)–C(2B)	1.26 (3)
N–C(5)	1.44 (4)	N(B)–C(5B)	1.48 (3)
C(1)–C(2)	1.41 (3)	C(1B)–C(2B)	1.46 (4)
C(2)–C(3)	1.53 (3)	C(2B)–C(3B)	1.50 (4)
C(3)–C(4)	1.52 (3)	C(3B)–C(4B)	1.54 (4)
C(4)–C(5)	1.55 (3)	C(4B)–C(5B)	1.53 (3)
Os–C(CO)	1.90 (3)*	C–O(CO)	1.15 (3)*
	Angles		
Os(1)–Os(2)–Os(3)	64.61 (3)	N–C(2)–C(3)	112 (2)
Os(1)–Os(3)–Os(2)	57.66 (3)	C(1)–C(2)–C(3)	125 (2)
Os(2)–Os(1)–Os(3)	57.73 (3)	C(2)–C(3)–C(4)	103 (2)
C(2)–N–C(5)	112 (2)	C(3)–C(4)–C(5)	103 (2)
N–C(2)–C(1)	123 (2)	N–C(5)–C(4)	105 (2)
Os–C–O(CO)	175 (3)*		

[a] Numbers in parentheses are estimated standard deviations in the least significant digits. Asterisks indicate average values.

Table V. Fractional Atomic Coordinates for $(\mu\text{-H})_2(\mu_3\text{-}\eta^2\text{-CH}\overline{\text{C=NCH}_2\text{CH}_2\text{C}}\text{H}_2)\text{Os}_3(\text{CO})_9$ (5)

atom	*x*	*y*	*z*	*B*,[a] Å^2
Os(1)	0.11186 (6)	0.36883 (6)	0.24275 (8)	1.16 (1)
Os(2)	0.32150 (7)	0.38327 (6)	0.15479 (8)	1.24 (2)
Os(3)	0.19837 (7)	0.47433 (6)	−0.02515 (8)	1.24 (2)
O(11)	−0.118 (1)	0.346 (1)	0.314 (2)	2.0 (3)*
O(12)	0.113 (1)	0.528 (1)	0.427 (2)	2.6 (3)*
O(13)	0.171 (1)	0.249 (1)	0.493 (2)	2.7 (3)*
O(21)	0.355 (1)	0.198 (1)	0.252 (2)	2.5 (3)*
O(22)	0.352 (1)	0.456 (1)	0.455 (2)	2.8 (3)*
O(23)	0.531 (1)	0.398 (1)	−0.028 (2)	2.4 (3)*
O(31)	0.086 (1)	0.430 (1)	−0.275 (2)	2.8 (3)*
O(32)	0.096 (1)	0.651 (1)	0.049 (2)	1.8 (3)*
O(33)	0.369 (2)	0.548 (1)	−0.244 (2)	3.2 (4)*
N	0.131 (1)	0.273 (1)	0.082 (2)	1.3 (3)*
C(1)	0.267 (2)	0.348 (2)	−0.049 (2)	1.5 (4)*
C(2)	0.199 (2)	0.281 (2)	−0.032 (2)	1.4 (3)*
C(3)	0.203 (2)	0.207 (2)	−0.141 (2)	1.6 (4)*
C(4)	0.104 (2)	0.165 (2)	−0.087 (2)	1.8 (4)*
C(5)	0.076 (2)	0.196 (2)	0.076 (3)	2.4 (4)*
C(11)	−0.031 (2)	0.359 (1)	0.282 (2)	1.1 (3)*
C(12)	0.107 (2)	0.467 (2)	0.362 (2)	1.3 (3)*
C(13)	0.150 (2)	0.300 (2)	0.396 (2)	1.2 (3)*
C(21)	0.342 (2)	0.268 (2)	0.213 (3)	2.0 (4)*
C(22)	0.345 (2)	0.434 (2)	0.336 (3)	2.2 (4)*
C(23)	0.453 (2)	0.395 (2)	0.049 (2)	1.4 (3)*
C(31)	0.124 (1)	0.450 (1)	−0.185 (2)	0.7 (3)*
C(32)	0.137 (2)	0.585 (1)	0.026 (2)	1.1 (3)*
C(33)	0.304 (2)	0.519 (2)	−0.164 (3)	2.0 (4)*
Os(1B)	0.21562 (6)	−0.16371 (6)	0.26843 (8)	1.20 (1)
Os(2B)	0.24375 (7)	−0.03262 (6)	0.49224 (8)	1.31 (2)
Os(3B)	0.37400 (6)	−0.05016 (6)	0.21852 (8)	1.16 (1)
O(11B)	0.046 (1)	−0.285 (1)	0.368 (2)	2.2 (3)*
O(12B)	0.079 (1)	−0.029 (1)	0.133 (2)	2.2 (3)*
O(13B)	0.304 (11)	−0.249 (1)	−0.029 (2)	2.1 (3)*
O(21B)	0.183 (1)	−0.117 (1)	0.795 (2)	2.9 (4)*
O(22B)	0.050 (2)	0.085 (2)	0.499 (2)	3.3 (4)*
O(23B)	0.362 (1)	0.107 (1)	0.609 (2)	2.2 (3)*
O(31B)	0.522 (1)	−0.186 (1)	0.073 (2)	2.2 (3)*
O(32B)	0.298 (1)	0.025 (1)	−0.063 (2)	2.3 (3)*
O(33B)	0.532 (1)	0.079 (1)	0.238 (2)	1.8 (3)*
N(B)	0.322 (1)	−0.237 (1)	0.375 (2)	1.2 (3)*
C(1B)	0.388 (2)	−0.105 (2)	0.435 (2)	1.3 (3)*
C(2B)	0.383 (2)	−0.199 (2)	0.440 (2)	1.7 (4)*
C(3B)	0.452 (2)	−0.261 (2)	0.509 (3)	2.3 (4)*
C(4B)	0.439 (2)	−0.347 (2)	0.434 (3)	2.2 (4)*
C(5B)	0.333 (2)	−0.332 (2)	0.389 (2)	1.6 (4)*
C(11B)	0.110 (2)	−0.242 (2)	0.332 (2)	1.6 (4)*
C(12B)	0.129 (2)	−0.080 (2)	0.181 (3)	2.0 (4)*
C(13B)	0.269 (2)	−0.216 (2)	0.084 (2)	1.3 (3)*
C(21B)	0.211 (2)	−0.087 (2)	0.681 (2)	1.3 (3)*
C(22B)	0.119 (2)	0.042 (2)	0.496 (3)	2.1 (4)*
C(23B)	0.316 (2)	0.055 (1)	0.569 (2)	1.1 (3)*
C(31B)	0.468 (2)	−0.134 (1)	0.124 (2)	1.1 (3)*
C(32B)	0.329 (1)	−0.001 (1)	0.042 (2)	0.7 (3)*
C(33B)	0.472 (2)	0.028 (2)	0.233 (2)	1.7 (4)*

[a] Starred *B* values are for atoms that were refined isotropically. Anisotropically refined atoms are given in the form of the isotropic equivalent displacement parameter defined as $(4/3)[a^2B(1,1) + b^2B(2,2) + c^2B(3,3) + ab(\cos\gamma)B(1,2) + ac(\cos\beta)B(1,3) + bc(\cos\alpha)B(2,3)]$.

= 2.808 (1) Å). The positions of the hydrides were calculated using HYDEX.[13] In molecule A the location of H(1), almost in the plane of the metal atoms, is consistent with the elongated Os(1)–Os(3) distance, and its location trans to CO(13) and CO(33) maintains octahedral geometry around Os(1) and Os(3). Similarly the position of H(2), trans to CO(21) and CO(31), places it 1.16 Å below the metal plane consistent with the shorter Os(2)–Os(3) bond distance, which is expected for a hydride bridging the same metal edge as another single bridging atom.[10,14,15,20] The bridging methyne carbon, C(1), donates two electrons to the metal core through similar metal–carbon σ bonds to Os(2) and Os(3), C(1)–Os(2) = 2.19 (2) and C(1)–Os(3) = 2.14 (2) Å. Two additional electrons are donated by the lone pair on nitrogen by a two-electron donor σ bond from N to Os(1) (N–Os(1) = 2.10 (2) Å) as for 4. The long C(2) to metal distances (C(2)–Os(1) = 2.92 (3), C(2)–Os(2) = 3.07 (3), and C(2)–Os(3) = 3.02 (3) Å) would seem to indicate that there is no appreciable bonding interaction with the metal core. Furthermore, the very short carbon–nitrogen double bond (C(2)–N = 1.28 (3) Å) would seem to discount any π-bonding interaction between this bond and the metal core. In both molecule A and molecule B the pyrrolidine ring tilts to the side toward the Os(3)–Os(1) edge by 8.7 and 6.4°, respectively, relative to the Os_3 plane. In molecule A the hydride (H(1)) is on the edge toward the tilt of the ring, while in molecule B the hydride (H(1B))

---

(20) Deeming, A. J.; Arce, A. J.; DeSanctis, Y.; Day, M. W.; Hardcastle, K. I. *Organometallics* 1989, *8*, 1408.

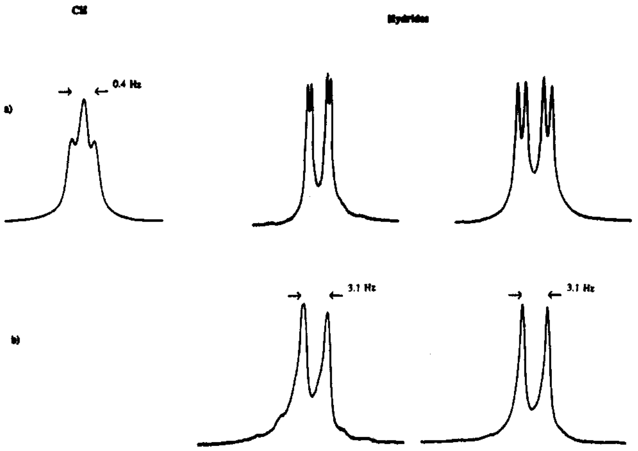

Figure 3. 360-MHz ^{1}H NMR of 4: (a) methyne and hydride origins at +22 °C; (b) hydride region with proton decoupling at the methyne hydrogen.

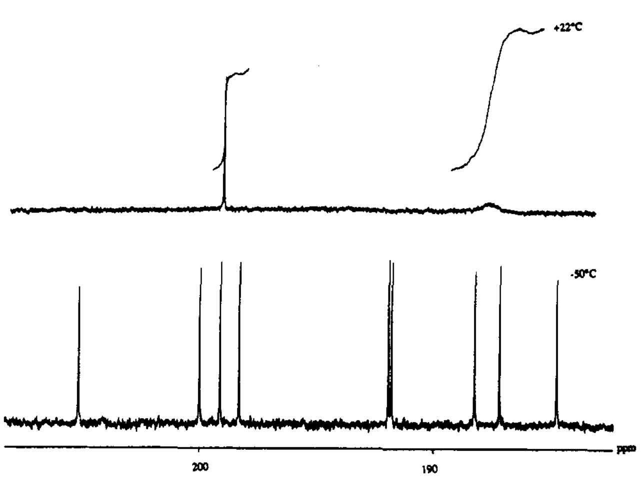

Figure 4. 90-MHz natural-abundance {H}^{13}C NMR of the carbonyl region of 4 at +22 and −50 °C.

is on the edge away from the tilt of the ring. It is interesting to note that the structure shows that the ring protons are inequivalent as evidenced by an approximate 9° tilt of the least-squares plane of the ring with respect to the least-squares plane of the metals.

The ^{1}H-NMR spectra of 4–6 share the common feature that the methyne proton exhibits coupling to the hydrides. In the case of 4 the methyne proton appears as a partially overlapping doublet of doublets (Figure 3) and the hydrides appear as two doublets of doublets (−12.49 ppm, ^2J(H–H) = 3.1, ^3J(H–H) = 0.6 Hz; −14.97 ppm, ^2J(H–H) = 3.1, ^3J(H–H) = 0.9 Hz; Figure 3). Irradiation of the methyne proton results in a collapse of the hydride signals to two doublets (Figure 3). Long-range couplings such as these between hydrocarbons and bridging hydrides in trimetallic clusters have been previously observed.[15] Interestingly, coupling to both hydrides is observed here even though H(1) is edge hopping from the Ru(3)–Ru(2) to the Ru(1)–Ru(2) edge. This is evidenced from the fact that the methylene protons in 4 appear as a slightly broadened quartet at +22 °C and an AB pattern at −50 °C and by the ^{13}C-NMR of the carbonyl region in which all but one carbonyl (presumably CO(22)) is broadened into the baseline at +22 °C while at −50 °C the expected nine carbonyls are observed (see Experimental Section and Figure 4). This type of edge hopping of one of two hydrides in trinuclear clusters has been previously observed.[15b] In order for coupling to be maintained, the rate constant for hydride edge hopping must be less $2\pi J$ or 3.8 s^{-1}, assuming the mobile hydride is the lower field resonance.[15] An estimate of the rate of hydride edge hopping can be obtained from the ^{13}C NMR data where two equatorial carbonyls at 188.24 and 187.17 appear to be just coalescing at +22 °C (Figure 4). Using the +22 °C as the coalescence temperature, a rate constant of 0.76 s^{-1} is estimated.[15b]

Similarly, the hydride at −14.56 ppm in 5 shows a small coupling to the slightly broadened methyne doublet appearing as a doublet of doublets (^2J(H–H) = 1.7 Hz, ^3J = 0.8 Hz), which collapses to a doublet upon irradiation of the methyne proton. The hydrides are rigid in 5 as evidenced by the observation of nine carbonyl resonances and individual multiplets for the ring protons at +22 °C (see Experimental Section). Compound 6 also exhibits coupling to the methyne proton, but here the low field hydride at −14.04 ppm appears as an overlapping doublet of doublets (^2J(H–H) = 1.6 Hz, ^3J(H–H) = 0.7 Hz), while the higher field hydride appears as doublet. If the assignment of the higher field hydride in 4 and 5 to H(2) is valid[15] for 6 as well, then this reversal in the magnitude of ^3J(H–H) may reflect a difference in the dihedral angles between Os(2)–Os(3)–H(2) and Os(2)–Os(3)–CH and/or between Os(3)–Os(1)–H(1) and Os(2)–Os(3)–CH brought about by the different steric requirements of cyclic and acyclic ligands in 5 and 6, respectively. As expected, couplings with the methyne proton in 4 are significantly larger than with 5 and 6.

The unexpectedly mild conditions under which 1–3 undergo reaction with diazomethane could arise from the presence of the highly fluxional μ_3-imidoyl ligand. The previously reported reactions of diazomethane with triosmium alkyne clusters utilized the coordinatively unsaturated 46e$^-$ cluster (μ_3-η^2-$C_6H_5C_2C_6H_5$)$Os_3(CO)_9$ (eq 10).[5]

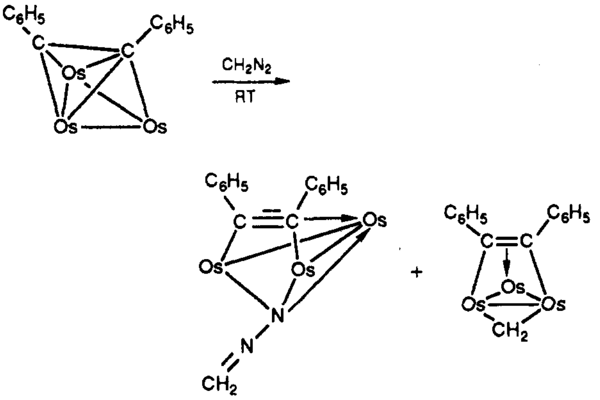

(10)

It occurred to us that the precursor to this 46e$^-$ species, (μ_3-η^2-$C_6H_5C_2C_6H_5$)$Os_3(CO)_{10}$, is also fluxional with respect to migration of the alkyne ligand and the bridging carbonyl. In fact we recently reported that the barrier to alkyne migration over the face of the cluster in the closely related complex (μ-CO)(μ_3-η^2-$CH_3C_2CH_3$)$Os_3(CO)_9$ (9)[21] was very similar to that observed in 2 and 3 (61 ∓ 4 kJ for 9, 56 ∓ 2 kJ for 2, and 55 ∓ 2 kJ for 3).[10,21] We thought it might, therefore, be possible to react 9 with diazomethane without proceeding through the 46e$^-$ intermediate. Indeed 9 slowly reacts with diazomethane to yield (μ-CH_2)(μ_3-η^2-$CH_3C_2CH_3$)$Os_3(CO)_9$ (10) in 59% yield and (μ_3-η^1-CH_2N_2)(μ_3-η^2-$CH_3C_2CH_3$)$Os_3(CO)_9$ (11) in 22% yield (eq 11). Interestingly, using the 48e$^-$ cluster 9, the methylene complex is the major product whereas the 46e$^-$ electron analog gives the diazomethane complex as the major product (eq 8). The difference in relative yields of

---

[21] Rosenberg, E.; Bracker-Novak, J.; Gellert, R. B.; Aime, S.; Gobetto, R.; Osella, D. J. *Organomet. Chem.* **1989**, *365*, 163.

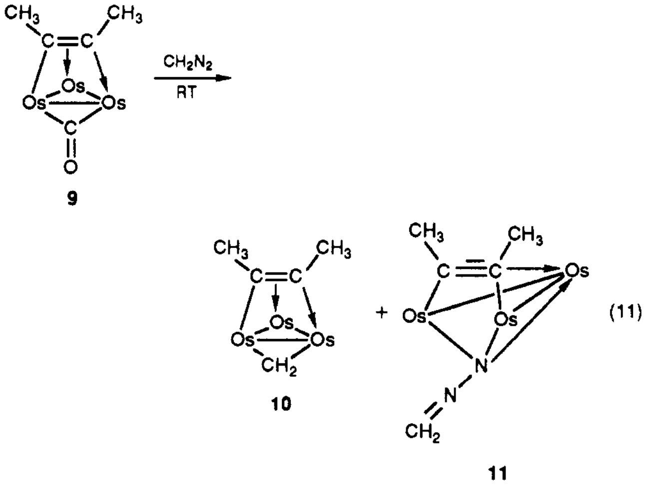

(11)

the methylene and diazomethane products between 7 and $Os_3(CO)_9(C_6H_5C_2C_6H_5)$ could be due to the different electron counts or the different alkyne substituents (C_6H_5 vs CH_3). Although the presence of the μ-CH_2 and the overall structure of **10** could be readily inferred from its ^1H NMR and infrared spectra, we decided to perform a solid-state structure of **10**, since the related starting materials $(\mu_3\text{-}\eta^2\text{-}C_6H_5C_2C_6H_5)Os_3(CO)_{10}$[22] and **9**[21,23] have distinctly different structures. The structure of **10** is shown in Figure 5, crystal data are given in Table I, and a few selected distances and angles are given in the caption. Unlike the alkyne clusters $(\mu_3\text{-}\eta^2\text{-}RC_2R)Os_3(CO)_{10}$ (R = CH_3,C_6H_5),[21-23] $(\mu\text{-}CH_2)(\mu_3\text{-}\eta^2\text{-}C_6H_5C_2C_6H_5)Os_3(CO)_9$[5] and **10** have virtually identical structures.

The structure of **11** is shown in Figure 6, selected distances and bond angles are given in the figure caption, and crystal data are given in Table I. The structure of **11** is virtually identical to that reported by Shapley and coworkers[5] in that the nitrogen atom is μ_3-bonded making **11** a 50e$^-$ cluster and resulting in opening of the Os(1)–Os(3) bond to a nonbonding distance of 3.685 (1) Å (eq 9). The overall geometry of the cluster can best be described as a pentagonal-based pyramid with Os(2) as the apex. The Os(1) and Os(3) bonds to carbon and nitrogen fall in a fairly narrow range (2.10 (1)–2.05 (1) Å), while the Os(3) bonds to acetylenic carbons are significantly longer (0.12 Å) than the Os(3) bond to nitrogen. The ^1H NMR of **11** in the methylene region shows an AB quartet at 5.87 and 5.89 ppm (J_{A-B} = 10.5 Hz). These data are almost identical with those reported for Shapley's diazomethane complex[5] (6.10 and 6.13 ppm, J_{A-B} = 10 Hz). Two other examples of μ_3-η^1-coordinated diazomethanes have been reported, $Cp_3Co_3(CO)(N_2CPh_2)$ and $Fe_3(CO)_9(N_2CPh_2)_2$.[24]

Thermolysis of **10** in refluxing octane for 6 h leads to isomerization to the σ-π-allyl complex $(\mu\text{-}H)(\mu_3\text{-}\eta^3\text{-}CH_3CC(CH_3)CH)Os_3(CO)_9$ (**12**) in high yield (eq 12) as observed for the diphenyl analog.[5] The relatively slow rate of carbon–carbon bond formation in **8** and its diphenyl analog is somewhat surprising in light of the close proximity the methylene and alkyne fragments on the trinuclear cluster and sharply contrasts with the room-temperature carbon–carbon bond-forming process observed in the reaction of **2** and **3** with diazomethane. In the absence of any knowledge of the initial intermediates leading to the formation **5** and **6**, these results are difficult to rationalize except to say that μ_3-imidoyl clusters are particularly reactive 48e$^-$ saturated clusters. We have also observed equally facile carbon–carbon coupling in the reactions of μ_3-imidoyl species with alkynes.[25] Further

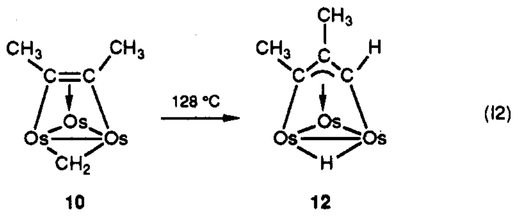

(12)

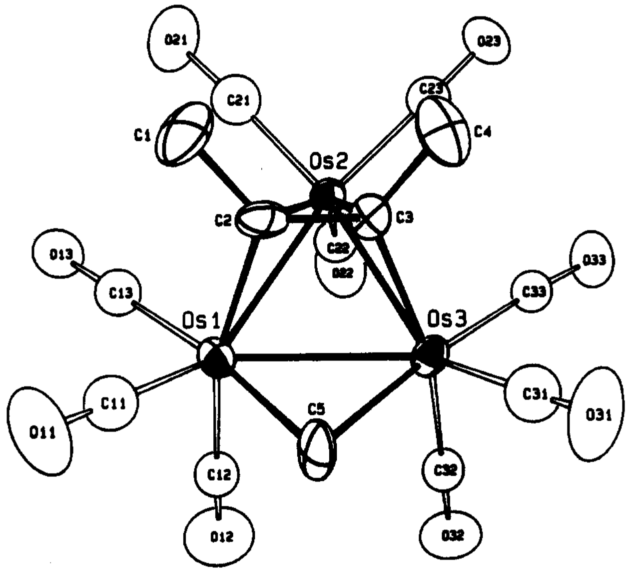

Figure 5. ORTEP diagram of $(\mu\text{-}CH_2)(\mu_3\text{-}\eta^2\text{-}CH_3C_2CH_3)Os_3(CO)_9$ (**10**). Selected distances (Å) and angles (deg) are as follows: Os(1)–Os(2) = 2.749 (1), Os(1)–Os(3) = 2.766 (1), Os(2)–Os(3) = 2.728 (1), Os(1)–C(5) = 2.15 (2), Os(3)–C(5) = 2.17 (2), Os(1)–C(2) = 2.14 (2), Os(3)–C(3) = 2.16 (2), Os(2)–C(2) = 2.27 (2), Os(2)–C(3) = 2.24 (2); Os(1)–C(5)–Os(3) = 79.7 (8), C(1)–C(2)–C(3) = 123 (2), C(2)–C(3)–C(4) = 125 (2).

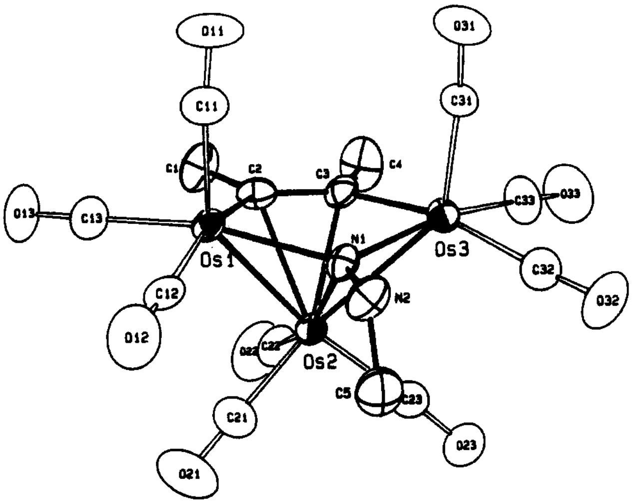

Figure 6. ORTEP diagram of $(\mu_3\text{-}\eta^1\text{-}CH_2N_2)(\mu_3\text{-}\eta^2\text{-}CH_3C_2CH_3)Os_3(CO)_9$ (**11**). Selected distances (Å) and angles (deg) are as follows: Os(1)–Os(2) = 2.779 (1), Os(2)–Os(3) = 2.795 (1), Os(1)–N(1) = 2.09 (1), Os(3)–N(1) = 2.05 (1), Os(2)–N(1) = 2.20 (1), N(1)–N(2) = 1.38 (1), N(2)–C(5) = 1.30 (2), Os(1)–Os(2)–Os(3) = 82.77 (2), Os(1)–N(1)–Os(3) = 125.8 (3), N(1)–N(2)–C(5) = 121.0 (1).

---

[22] (a) Shapley, J. R.; Tachikawa, M.; Pierpont, C. G. *J. Am. Chem. Soc.* **1975**, *97*, 7172. (b) Pierpont, C. G. *Inorg. Chem.* **1977**, *16*, 636.

[23] Gallop, M. A.; Johnson, B. F. G.; Khattar, R.; Lewis, J.; Raithby, P. *J. Organomet. Chem.* **1990**, *386*, 121.

[24] (a) Bagga, M. M.; Balie, P. E.; Mill, O. S.; Pauson, P. L. *J. Chem. Soc., Chem. Commun.* **1967**, 1106. (b) Hermann, W. A. *Angew. Chem., Int. Ed. Engl.* **1978**, *17*, 800.

[25] Day, M.; Kabir, S. E.; Hardcastle, K. I.; Rosenberg, E. Unpublished results.

studies with substituted diazoalkenes where α-carbon–hydrogen bond activation can be precluded in the hope of isolating some earlier intermediates on the way to forming 5 and 6 are currently under investigation.

Experimental Section

General Procedures. All reactions were carried out under an atmosphere of nitrogen, unless stated otherwise. Methylene chloride was distilled from calcium hydride prior to use. Diethyl ether was dried over 4-Å molecular sieves and degassed by purging with nitrogen before use. 2-(2-Ethoxyethoxy)ethanol, *N*-methyl-*N*-nitroso-*p*-toluenesulfonamide, and *N*-methyl-d_3-*N*-nitroso-*p*-toluenesulfonamide were purchased from Aldrich and used as received. Infrared spectra were recorded on a Perkin-Elmer 1420 spectrophotometer. ^{1}H NMR spectra were obtained on a Bruker AM-400, Bruker AMX-360, or IBM-NR80 spectrometer. Elemental analyses were performed by Schwarzkopf Microanalytical Laboratory, New York.

Diazomethane[26] and deuterated diazomethane[27] were prepared according to the known procedures. The clusters (μ-H)(μ_3-η^2-$CH_3C{=}NCH_2CH_3$)$Ru_3(CO)_9$,[9] (μ-H)(μ-η^2-$CH_3C{=}NCH_2CH_3$)$Ru_3(CO)_{10}$,[12] (μ-H)(μ_3-η^2-$CH_3CH_2C{=}NCH_2CH_2CH_3$)$Os_3(CO)_9$,[10] ($\mu$-H)($\mu_3$-$\eta^2$-$\overline{C{=}NCH_2CH_2C}H_2$)$Os_3(CO)_9$,[10] and ($\mu$-CO)($\mu_3$-$\eta^2$-$CH_3C_2CH_3$)$Os_3(CO)_9$[28] were prepared by the literature procedures.

Reaction of (μ-H)(μ_3-η^2-$CH_3C{=}NCH_2CH_3$)$Ru_3(CO)_9$ (1) with Diazomethane. An ether solution of diazomethane (70 mL, ~16.6 mmol) was distilled into an ether solution of 1 (0.294 g, 0.469 mmol) at 0 °C from the diazomethane generator. Immediate formation of insoluble polymethylene was observed. The color of the solution changed from yellow to orange-red. After stirring for about 4 h at 0 °C, the reaction mixture was allowed to warm to room temperature and the solvent and excess diazomethane was removed by blowing nitrogen through the solution. The residue was extracted with methylene chloride, an the extract was filtered and chromatographed by preparative TLC on silica gel. Elution with hexane/CH_2Cl_2 (6:1, v/v) resolved two bands. The fastest moving (orange) band yielded (μ-H)(μ_3-η^2-$CH(CH_3)C{=}NCH_2CH_3$)$Ru_3(CO)_9$ (4) as orange crystals (0.091 g, 90% based on consumed 1) after recrystallization from hexane at −20 °C. The second band gave unreacted 1 (0.190 g). All attempts to optimize the yield of 4 including the addition of 1 to an excess of diazomethane and addition of aliquots of diazomethane to a solution of 1 in different solvents (e.g. hexane, benzene, methylene chloride, and diethyl ether) at various temperatures (0–80 °C) were unsuccessful, and in every case formation of a large amount of polymethylene was observed.

Spectral and Analytical Data for 4: IR (ν(CO) in hexane) 2093 w, 2065 s, 2041 vs, 2024 w, 2017 s, 1996 s, 1982 w, 1974 w cm^{-1}; 400-MHz ^{1}H NMR (in CD_2Cl_2 at −20 °C, low-temperature limit) 4.63 (s, 1 H), 3.18 (m, 1 H), 3.08 (m, 1 H), 1.87 (s, 3 H), 0.95 (t, 3 H, J_{H-H} = 7.2 Hz), −12.49 (dd, 1 H, $^2J_{H-H}$ = 3.1 Hz, $^3J_{H-H}$ = 0.6 Hz), −14.97 (dd, 1 H, $^2J_{H-H}$ = 3.1 Hz, $^3J_{H-H}$ = 0.9 Hz) ppm; 90-MHz {H}^{13}C NMR (CD_2Cl_2, −50 °C, carbonyl region) 208.67 (s, *C*=N1C), 205.19 (s, 1 C), 200.02 (s, 1 C), 199.14 (s, 1 C) 198.33 (s, 1 C), 191.93 (s, 1 C), 191.79 (s, 1 C), 188.24 (s, 1 C) 187.17 (s, 1 C), 184.73 (s, 1 C). Polymeric residue IR (KBr): 2919 (s), 2850 (s), 1473 (m), 719 (m) cm^{-1}. Anal. Calcd for $C_{14}H_{11}NO_9Ru_3$: C, 26.25; H, 1.73; N, 2.19. Found: C, 26.32; H, 1.60; N, 2.10.

Reaction of (μ-H)(μ-η^2-$CH_3C{=}NCH_2CH_3$)$Ru_3(CO)_{10}$ with Diazomethane. An ethereal solution of diazomethane (70 mL, ~16.6 mmol) was distilled into a methylene chloride solution (30 mL) of (μ-H)(μ-η^2-$CH_3C{=}NCH_2CH_3$)$Ru_3(CO)_{10}$ (0.160 g, 0.244 mmol) at 0 °C. The color of the reaction mixture immediately changed from orange to red. No polymer formation was observed even after 1 h. The reaction mixture was then warmed to room temperature and allowed to stand for 24 h, during which time slow polymer formation was observed. The solution was filtered, and the solvent from the filtrate was removed under reduced pressure to give a red-brown residue, which was dissolved in a minimum volume of methylene chloride and chromatographed by TLC on silica gel. The residue from this extraction was an off-white solid (90 mg). Elution with hexane/CH_2Cl_2 (6:1, v/v) gave two main bands. The faster moving band gave 4 (0.028 g, 50% based on consumed 1), while the second band yielded 1 (0.070 g, 46%).

Reaction of 1 with Deuterated Diazomethane. An ethereal solution of deuterated diazomethane (30 mL, ~4.1 mmol) was distilled into an ethereal solution (25 mL) of 1 (0.224 g, 0.358 mmol) at 0 °C. After stirring for 4 h, the solution was filtered and the solvent was removed under vacuum. The ^{1}H NMR of the crude product in $CDCl_3$ clearly indicated ~50% deuterium incorporation only into both hydride positions of 4 and no incorporation of a proton into the methyne position. After the ^{1}H NMR was recorded, the crude product was separated by preparative TLC plates as above. The ^{1}H NMR spectrum of the isolated product showed ~50% deuterium incorporation into both hydride positions of 4.

Reaction of (μ-H)(μ_3-η^2-$\overline{C{=}NCH_2CH_2C}H_2$)$Os_3(CO)_9$ with Diazomethane. To a methylene chloride solution (10 mL) of 2 (0.110 g, 0.123 mmol) were added 2-mL aliquots of a freshly prepared diazomethane solution in ether (~0.2 M) for every 30 min for a total of 4 h, during which time the slow formation of polymethylene was observed. The solution was filtered, and the solvent from the filtrate was removed by blowing nitrogen through the solution. TLC separation of the residue eluting with hexane/CH_2Cl_2 (10:3, v/v) gave two bands. The faster moving band gave (μ-H)$_2$(μ_3-η^2-$CH\overline{C{=}NCH_2CH_2C}H_2$)$Os_3(CO)_9$ (5) as orange crystals (0.011 g, 75% based on consumed 2) after recrystallization from hexane/CH_2Cl_2 at −20 °C. The slowest moving band gave unconsumed 2 (0.095 g). All attempts to optimize the yield of 5 as described above for 4 were unsuccessful.

Spectral and Analytical Data for 5: IR (ν(CO) in hexane) 2097 w, 2069 s, 2056 w, 2043 s, 2011 s, 1997 m, 1998 m, 1970 m cm^{-1}; 400-MHz ^{1}H NMR (in C_6D_6) 3.84 (s, 1 H), 2.64 (m, 1 H), 2.41 (m, 1 H), 1.52 (m, 1 H), 1.29 (m, 1 H), 1.10 (m, 1 H), 0.96 (m, 1 H), −14.30 (d, 1 H, J_{H-H} = 1.7 Hz), −14.56 (dd, 1 H, $^2J_{H-H}$ = 1.7 Hz, $^3J_{H-H}$ = 0.8 Hz) ppm; 90-MHz {H}^{13}C NMR ($CDCl_3$, +22 °C, carbonyl region) 218.07 (s, *C*=N), 183.33 (s, 1 C), 179.24 (s, 1 C), 177.56 (s, 1 C), 175.73 (s, 1 C), 172.00 (s, 1 C), 171.68 (s, 1 C), 168.45 (s, 1 C), 166.49 (s, 1 C), 161.44 (s, 1 C). Anal. Calcd for $C_{14}H_9NO_9Os_3$: C, 18.56; H, 1.00; N, 1.55. Found: C, 18.41; H, 1.01; N, 1.43.

Reaction of (μ-H)(μ_3-η^2-$CH_3CH_2C{=}NCH_2CH_2CH_3$)$Os_3(CO)_9$ (3) with Diazomethane. A methylene chloride solution (10 mL) of 3 (0.040 g, 0.043 mmol) was added to an ethereal solution of diazomethane (70 mL, ~16.6 mmol). The color of the solution changed from pale yellow to yellow. The reaction mixture was allowed to stir at room temperature for 24 h over which time slow formation of polymethylene was observed. The polymer was separated by filtration, and the solvent from the filtrate was removed by blowing nitrogen through the solution. The residue was dissolved in a minimum volume of methylene chloride and applied to a silica gel TLC plate. Elution with hexane/CH_2Cl_2 (4:1, v/v) resolved two bands. The faster moving band afforded (μ-H)$_2$(μ_3-η^2-$CH(CH_3CH_2)C{=}NCH_2CH_2CH_3$)$Os_3(CO)_9$ (6) as yellow crystals (0.007 g, 54% based on consumed 3) from hexane/CH_2Cl_2. The slowest moving band gave unreacted 3 (0.030 g).

Spectral and Analytical Data for 6: IR (ν(CO) in hexane) 2096 w, 2068 s, 2042 s, 2011 s, 1996 m, 1984 m, 1967 m cm^{-1}; 400-MHz ^{1}H NMR (in $CDCl_3$) 4.66 (s, 1 H), 3.34 (m, 1 H), 3.22 (m, 1 H), 2.12 (m, 1 H), 2.02 (m, 1 H), 1.41 (m, 2 H), 1.19 (t, 3 H, J_{H-H} = 7.6 Hz), 0.88 (t, 3 H, J_{H-H} = 7.5 Hz), −14.04 (two partially overlapping doublets, 1 H, J_{H-H} = 1.5 Hz), −14.59 (d, 1 H, J_{H-H} = 1.5 Hz) ppm. Anal. Calcd for $C_{16}H_{15}NO_9Os_3$: C, 20.53; H, 1.62; N, 1.50. Found: C, 20.55; H, 1.69; N, 1.55.

Synthesis of 5 from 2-Methylpyrrolidine and $Os_3(CO)_{10}(CH_3CN)_2$. To a benzene solution (250 mL) of $Os_3(CO)_{10}(CH_3CN)_2$ prepared from 506 mg of $Os_3(CO)_{12}$ (0.56 mmol) was added 0.275 mL (2.6 nmol) of 2-methylpyrrolidine, and the solution was warmed to 50 °C for 5 h under a slow nitrogen flow. The resulting yellow-orange solution was evaporated to dryness, the solid was taken up in methylene chloride, and the mixture was subjected to thin-layer chromatography on silica using 20:80

---

(26) DeBoer, T. J.; Backer, H. J. *Org. Synth.* **1956**, *36*, 16.
(27) Campbell, J. R. *Chem. Int.* **1972**, 540.
(28) Johnson, B. F. G.; Khattar, R.; Lewis, J.; Raithby, P. R.; Smit, D. N. *J. Chem. Soc., Dalton Trans.* **1988**, 1421.

methylene chloride/hexane as eluent. Two major yellow bands eluted. The faster moving band proved to be $(\mu\text{-H})Os_3(CO)_{10}(\mu\text{-}\eta^2\text{-}\overline{C{=}NCH(CH_3)CH_2C}H_2)$ (7) (96 mg 18%), and the slower moving band proved to be $(\mu\text{-H})(\mu\text{-}\eta^2\text{-}CH_2\overline{C{=}NCH_2CH_2C}H_2)Os_3(CO)_{10}$ (8) (33 mg, 8%).

Compound 8 (30 mg, 0.03 mmol) was thermalized in 10 mL of refluxing *n*-heptane (98 °C) for 23 h at which time complete conversion to 5 was noted by analytical thin-layer chromatography. After evaporation of solvent essentially quantitative recovery of 5 was realized.

Spectral Data for 7 and 8. Data for 7: IR (ν(CO) in hexane) 2101 m, 2060 s, 2049 s, 2022 s, 2003 s, 1988 s, 1975 m, 1950 w cm^{-1}; 360 MHz ^{1}H NMR ($CDCl_3$, two isomers) isomer a (60%) 3.72 (m, 1 H), 2.60 (m, 1 H), 2.36 (m, 1 H), 2.01 (m, 1 H), 1.24 (m, 1 H), 1.19 (d, 3 H, $J_{H\text{-}H}$ = 6.7 Hz), −15.55 (s, 1 H) ppm; isomer b (40%) 3.61 (m, 1 H), 2.60 (m, 1 H), 2.28 (m, 1 H), 2.01 (m, 1 H), 1.24 (m, 1 H), 1.21 (d, 3 H, $J_{H\text{-}H}$ = 6.6 Hz), −15.53 (s, 1 H) ppm. Anal. Calcd for $C_{15}H_9NO_{10}Os_3$: C, 19.2; H, 0.97; N, 1.50. Found: C, 19.42; H, 1.10; N, 1.45. Data for 8: IR (ν(CO) in hexane) 2098 m, 2057 s, 2045 s, 2019 s, 1999 m, 1989 s, br, 1970 m cm^{-1}; 360-MHz ^{1}H NMR ($CDCl_3$) 3.84 (m, 1 H), 3.60 (m, 1 H), 2.71 (m, 1 H), 2.53 (m, 1 H), 2.18 (dm, 1 H, $J_{H\text{-}H}$ = 18.0 Hz), 1.97 (m, 2 H), 1.80 (dm, 1 H, $J_{H\text{-}H}$ = 18.0 Hz), −14.60 (d, 1 H, $J_{H\text{-}H}$ = 0.6 Hz, coupled to H at 2.18 ppm).

Reaction of $(\mu\text{-CO})(\mu_3\text{-}\eta^2\text{-}CH_3C_2CH_3)Os_3(CO)_9$ (9) with Diazomethane. To an ether solution (5 mL) of 9 (0.100 g, 0.110 mmol) was added 10 mL of an approximately 0.2 M ether solution of diazomethane. After the solution was stirred for 12 h at room temperature, the solvent was removed under reduced pressure and the residue was chromatographed by preparative TLC on silica gel. Elution with hexane/CH_2Cl_2 (5:1, v/v) gave three bands. The faster moving band gave $(\mu\text{-}CH_2)(\mu_3\text{-}\eta^2\text{-}CH_3C_2CH_3)Os_3(CO)_9$ (8) as orange crystals (0.024 g, 59% based on consumed 9) after recrystallization from hexane/CH_2Cl_2 at −20 °C. The second band gave unreacted 9 (0.050 g). The third band gave $(\mu_3\text{-}\eta^1\text{-}N_2CH_2)(\mu_3\text{-}\eta^2\text{-}CH_3C_2CH_3)Os_3(CO)_9$ (11) as yellow crystals (0.011 g, 22% based on consumed 9) after recrystallization from hexane/CH_2Cl_2 at −20 °C.

Spectral and Analytical Data for 10 and 11. Data for 10: IR (ν(CO) in hexane) 2090 m, 2052 vs, 2016 vs, 2004 s, 1992 s, 1984 sh cm^{-1}; 80–MHz ^{1}H NMR (in CD_2Cl_2) 7.98 (d, 1 H, $J_{H\text{-}H}$ = 5.1 Hz), 7.26 (d, 1 H, $J_{H\text{-}H}$ = 5.1 Hz), 2.34 (s, 6 H) ppm. Anal. Calcd for $C_{14}H_8O_9Os_3$: C, 18.87; H, 0.91. Found: C, 18.95; H, 1.05. Data for 11: IR (ν(CO) in hexane) 2092 w, 2076 w, 2065 s, 2058 w, 2044 m, 2006 vs, 1990 m, 1978 w, 1958 w, 1945 w cm^{-1}; 360-MHz ^{1}H NMR (in $CDCl_3$) 5.87 and 5.89 (AB quartet, $J_{A\text{-}B}$ = 10.5 Hz), 2.76 (s, 6 H) ppm. Anal. Calcd for $C_{14}H_8N_2O_9Os_3$: C, 18.30; H, 0.88; N, 3.05. Found: C, 18.38; H, 0.89; N, 3.09.

Thermolysis of 10. An octane solution (20 mL) of 10 (0.060 g, 0.067 mmol) was refluxed for 6 h. The solvent was removed under reduced pressure and the residue chromatographed by TLC on silica gel. Elution with hexane gave two bands. The fast moving band gave $(\mu\text{-H})(\mu_3\text{-}\eta^3\text{-}CH_3CC(CH_3)CH)Os_3(CO)_9$ (12) as pale yellow crystals (0.020 g, 80% based on the amount of 10 consumed) after recrystallization from hexane/CH_2Cl_2 at −20 °C, while the second band gave unreacted 10 (0.035 g).

Spectral and Analytical Data for 12: IR (ν(CO) in hexane) 2089 m, 2064 s, 2059 s, 2043 vs, 2034 s, 2014 s, 1999 vs, 1957 m, 1914 w cm^{-1}; 80-MHz ^{1}H NMR (in $CDCl_3$) 8.79 (s, 1 H), 2.86 (s, 3 H), 2.51 (s, 3 H), −19.22 (s, 1 H) ppm. Anal. Calcd for $C_{14}H_8O_9Os_3$: C, 18.87; H, 0.91. Found: C, 19.00; H, 0.93.

Photolysis of 11. A hexane solution (20 mL) of 11 (0.020 g, 0.022 mmol) in a 100-mL quartz tube was photolyzed using a Rayonet photochemical reactor irradiating with 3000-Å lamps for 15 min. The solvent was removed under reduced pressure and the residue chromatographed by TLC eluting with hexane to give 10 (0.005 g, 25%).

X-ray Structure Determination of 4, 5, 10, and 11. Crystals of 4, 5, 10, and 11 for X-ray examination were obtained from saturated solutions of each in hexane at −20 °C for 4 and 5 and a dichloromethane/hexane solvent system at −20 °C for 10 and 11. Suitable crystals of each were mounted on glass fibers, placed in a goniometer head on an Enraf-Nonius CAD4 difractometer, and centered optically. Unit cell parameters and an orientation matrix for data collection were obtained using the centering program in the CAD4 system. Details of the crystal data are given in Table I. For each crystal the actual scan range was calculated by scan width = scan range + 0.35 tan θ and backgrounds were measured using the moving crystal–moving counter techniques at the beginning and end of each scan. As a check on instrument and crystal stability three representative reflections for 4 and 5 and two reflections for 10 and 11 were measured every 2 h. Lorentz, polarization, and decay corrections were applied as was an empirical absorption correction based on a series of ψ scans. For 5 the empirical absorption correction method of Walker and Stuart (DIFABS) was used.[31]

Each of the structures was solved by the Patterson method using SHELXS-86, which revealed the positions of the metal atoms. All other non-hydrogen atoms were found by successive difference Fourier syntheses. The expected hydride positions were calculated using the program Hydex[13] and included in the structure factor calculations but not refined in the final least-squares cycles. Hydrogen atoms were not included in the calculations for structures 4, 10, and 11 but pyrrolidine hydrogen atom positions were determined in 5 and included as riding atoms. Final refinement parameters for each crystal are listed in Table I. Selected bond distances and angles for compounds 4 and 5 are given in Tables II and III. The rather large peaks in the final difference maps for 5 and 10 were not due to incorporated solvent molecules. The highest peaks were in and around the ring osmium atoms and most likely result from poorer crystal quality and/or uncorrected absorption effects.

Scattering factors were taken from Cromer and Waber.[29] Anomalous dispersion corrections were those of Cromer.[30] All calculations were carried out on a DEC MicroVAX II computer using the SDP/VAX system of programs.

Acknowledgment. We gratefully acknowledge the National Science Foundation (Grant CHE-9016495) and the donors of the Petroleum Research Foundation, administered by the American Chemical Society, for support of this research. We thank the National Science Foundation for a matching funds grant for purchase of a 360-MHz NMR spectrometer. We also thank Prof. A. Frateillo and R. Perrigan for help in obtaining 400-MHz ^{1}H NMR spectra at California State University, Los Angeles.

Supplementary Material Available: Atomic positions for 10 and 11 (Tables 7 and 8), anisotropic displacement factors (Tables 9–12), and complete bond distances and angles (Tables 13–16) (46 pages). Ordering information is given on any current masthead page.

OM910601M

---

(29) Cromer, D. T.; Waber, J. T. *International Tables for Crystallography*; Kynoch Press: Birmingham, England, 1974; Vol. IV, Table 2.2B.

(30) Cromer, D. T. *International Tables for Crystallography*; Kynoch Press: Birmingham, England, 1974; Vol. IV, Table 2.3.1.

(31) Walker, N.; Stuart, D. *Acta Crystallogr., Sect. A*, 1983, *39*, 1959.